http://www.e-journals.in
DOI:10.7598/cst2014.920

Chemical Science Transactions
2014, **3(4),** 1488-1496

RESEARCH ARTICLE

Microwave Assisted Synthesis, Characterization and Photocatalytic Activity of $Zn_2V_2O_7$ Nanospheres

S. DANIEL ABRAHAM[1], S. THEODORE DAVID[1*], R. BIJU BENNIE[a], C. JOEL[1], M. SEETHALAKSHMI[1] and T. ADINAVEEN[2]

[1]P.G. Department of Chemistry, St. John's College, Tirunelveli-627002, India
[2]Catalysis and Nanomaterials Research Laboratory, Loyola College, Chennai-600034, India
s.theodore.david@gmail.com

Received 29 July 2014 / Accepted 18 August 2014

Abstract: Zinc vanadate ($Zn_2V_2O_7$) nanoparticles have been synthesized successfully by simple microwave assisted combustion method using diethylene glycol as fuel. The structure and morphology of the synthesized zinc vanadate have been investigated by X-ray diffraction (XRD), Fourier transform infrared spectra (FT-IR), Raman Spectra, high resolution scanning electron microscopy (HR-SEM), Energy Dispersive X-ray analysis (EDX), diffused reflectance spectroscopy (DRS) and Photoluminescence studies(PL). The XRD reveals that the formation of monoclinic structure of $Zn_2V_2O_7$ whereas the formation of $Zn_2V_2O_7$ phase is confirmed by FT-IR spectra and Raman Spectra. HR-SEM confirms the formation of spherical hollow nanospheres. The optical properties were determined by UV-DRS and PL studies. The synthesised $Zn_2V_2O_7$ has been found to show superior photocatalytic activity in the photodegradation of malachite green (MG) dye.

Keywords: Microwave combustion synthesis, Optical studies, Zinc vanadate, Nanospheres

Introduction

Over the past decade, the shape control of anisotropic nano- and microcrystals has attracted extensive importance because the morphology, dimensionality and size of materials have great effects on their physical and chemical properties, as well as on their applications in various fields.[1,2] The shape control of semiconductor nanostructures play very significant roles in determining their physical and chemical properties.[3-4] Oxide and sulphide semiconductor materials with large band gap, such as TiO_2, WO_3, ZnO, CuO, ZrO_2, CdS, ZnS, *etc*., are commonly used as photocatalysts.[5] The efficiency of the photocatalytic processes depends upon the life time of the photo-generated electron/hole pairs[6]. Recently, there is a growing interest in the study of low-dimensional oxide nanomaterials, due to their potential applications in nanodevices. Metal vanadates, as one of the most important family of functional materials, have numerous applications in the fields of catalysts,[7] optical devices,[8] magnetic materials,[9] as well as battery materials.[10–12]

Microwave assisted combustion synthesis is becoming an increasingly popular and versatile method for the preparation of metal oxide nanoparticles, has shown significant advantages over conventional methods. Since, the microwave interaction is at a molecular level, the temperature distribution is homogeneous inside the solution causing an explosion reaction followed by vigorous evolution of gases to form nanostructures. The reaction can be performed in a domestic microwave oven and the operation is clean, fast, cheap. The prepared metal oxide nanoparticles are highly pure and the yield is also good. The reaction is completely done in aqueous medium and therefore no harmful organic solvents are used.[13-15] The advantages of microwave synthesis include unique microstructure and properties, improved product yield, energy savings, reduction in manufacturing cost and synthesis of new materials.[16] The novel precursors and synthetic routes will be more useful, which provides a new way for preparing nano materials to control shape, crystalline, and size distribution.[17] The materials with spherical shape morphology can find wide applications in photo catalysis for industrial waste pollutants, dyes and toxic compounds and also good ion exchanger capability in analytical chemistry, hydrometallurgy, separation of radioisotopes, water treatment and pollution control.[18-20]

In the present study, we have investigated a simple and rapid microwave assisted combustion route to synthesize spherical hollow zinc vanadate nanospheres using ethylene glycol as fuel. The whole process takes only a few minutes to yield zinc vanadate microspheres. The structure, morphology and optical properties of the synthesized zinc vanadate microspheres have been investigated by XRD, FT-IR, Raman, SEM with EDX, DRS and PL spectra. In addition, the photo catalytic degradation (PCD) ability of zinc vanadate in the malachite green has been investigated.

Experimental

All the chemicals were obtained from Merck, India (Analytical grade), and were used as such without further purification. About 0.5 mmol of zinc chloride (0.098 g) and 1mmol (0.116 g) of ammonium meta vanadate were dissolved in 15 mL diethylene glycol and 15 mL of deionized water, respectively. Then the mixture was heated to 110 °C for 3 min and then kept inside the microwave-oven (2.45 GHz and 750 W) for 5 min. After the completion of the reaction, the obtained solid was cooled naturally then washed with deionized water and absolute ethanol followed by drying at 110 °C for overnight.

Characterization of zinc vanadate photocatalyst

The structural characterization of zinc vanadate was performed using a Philips X'pert X-ray diffractometer with CuKα radiation at λ = 1.5056A°. The surface functional groups of zinc vanadate were analyzed by Perkin Elmer FT-IR spectrometer and the Raman scattering experiment was performed by EZ Raman, Enwave optronics Raman spectrometer. The morphological studies and energy dispersive X-ray analysis of zinc vanadate have been performed with a Jeol JSM6360 high resolution scanning electron microscope. The diffuse reflectance spectrum of zinc vanadate was recorded using Cary 100 UV–Visible spectrophotometer to estimate their energy band gap. The emission spectrum of zinc vanadate was performed using Varian Cary Eclipse Fluorescence Spectrophotometer. The extent of dye degradation was monitored by using UV−Vis spectrophotometer (Perkin-Elmer, Lamda 25).

Photocatalytic reactor and degradation procedure

PCD experiments were carried out in a self-designed photocatalytic reactor[17]. The cylindrical photocatalytic reactor tube was made up of borosilicate with a dimension of 36-1.6 cm

(height-diameter). The top portion of the reactor tube has ports for sampling, gas purging, and gas outlet. The aqueous MG solution containing appropriate quantity of $Zn_2V_2O_7$ was taken in the quartz/borosilicate tube and subjected to aeration for thorough mixing. This was then placed inside the reactor setup. The lamp housing has low pressure mercury lamps (8 x 8W) emitting 365 nm with polished anodized aluminium reflectors and black cover to prevent UV leakage. The PCD was carried out by mixing 100 mL of aqueous MG solution and fixed weight of $Zn_2V_2O_7$ photocatalyst. Prior to irradiation, the slurry was aerated for 30 min to reach adsorption equilibrium followed by UV irradiation. Aliquots were withdrawn from the suspension at specific time intervals and centrifuged immediately at 1500 rpm. The extent of MG degradation was monitored by using UV–Visible spectrophotometer (Perkin–Elmer, Lamda 25). The PCD efficiency(%) was calculated from the following expression,

$$\eta = Ci- Ct/Ci \times 100$$

Where, Ci is the initial concentration of MG and Ct concentration of MG after 't' minutes.

Results and Discussion

X-ray diffraction analysis

The structural phases of the zinc vanadate were determined by X-ray diffraction pattern. The XRD patterns were recorded for synthesized sample shown in Figure 1. The observed diffraction peaks at 2θ = 28.7579, 25.9544, 56.5379, and 33.8158° are associated with [0 2 2], [2 0 0], [1 3 4], and [2 2 2], plane, respectively. These planes are related with the d-spacing values of 3.10, 3.43, 1.56, and 2.65 Å. This clearly indicates the monoclinic phase of $Zn_2V_2O_7$ (JCPDS No. 70-1532). Furthermore, no characteristic peaks from other crystalline impurities were detected by XRD, indicating the high purity of zinc vanadate. The lattice parameter of synthesized sample is found to be a = 0.742, b = 0.834 nm and c = 1.009 nm. The average size of the particles was calculated using Scherrer formula[8] is

$$L = 0.89/ \beta \cos\theta$$

Where L is the crystallite size, λ, the X-ray wavelength, θ, the Bragg diffraction angle and β, the peak width at half maximum (PWHM). The average crystallite size 'L' calculated from the (0 2 2) diffraction peak was found to be 18 nm. The molecular weight of $Zn_2V_2O_7$ was found to be 344.64.

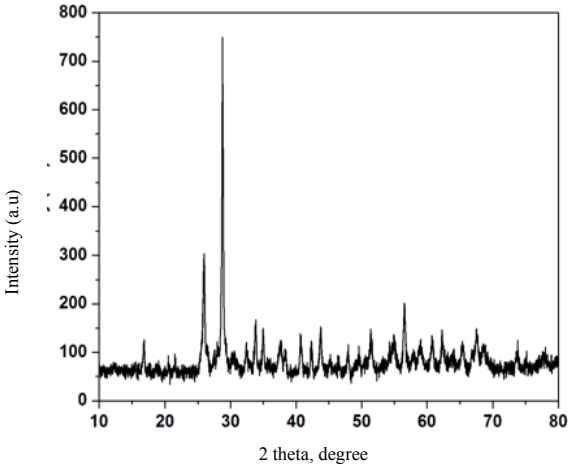

Figure 1. X-Ray diffraction of nano zinc vanadate

Infrared spectral analysis

The FT-IR spectrum of nano zinc vanadate is shown in Figure 2. The spectrum exhibits a common broad band near 3480 cm^{-1} due to the OH-stretching vibrations of free and hydrogen-bonded hydroxyl groups, and a second typical absorption region at 1630 cm^{-1} is assigned to the deformative vibration of water molecules, which is most probably due to water adsorption during the compaction of the powder specimens with KBr, The formation of ZnO phase present in tetrahedron unit of vanadates is characterized by an intense and very broad IR band with poor resolved shoulders at 580, 1400 and 1428 cm^{-1}.[9]

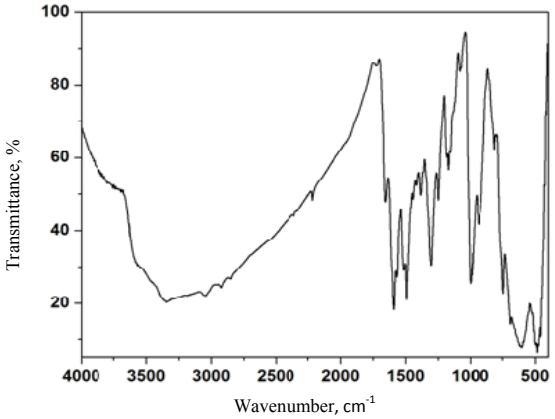

Figure 2. FT-IR Spectra of zinc vanadate

Raman spectral analysis

Raman scattering spectrum of zinc vanadate (ZnV_2O_7) is shown in Figure 3. The Raman peaks match with the IR spectral values and it's assigned to their vanadate (VO_4^{3-}) formation. The Raman peaks at 958, and 858 cm^{-1} are assigned to the V-O stretching mode, while bands at 624 cm^{-1} is assigned to the asymmetric stretching of the V–O. The band at 498 cm^{-1} is assigned to the symmetric stretching of the O–V–O, while the band at 312cm^{-1} allocated to asymmetric bending vibrations of O-V-O. The Raman peaks of the low-frequency region in 216 cm^{-1} related to the external vibrations, *i.e.* crystal lattice translational (T) and rotational (R) modes[10,12].

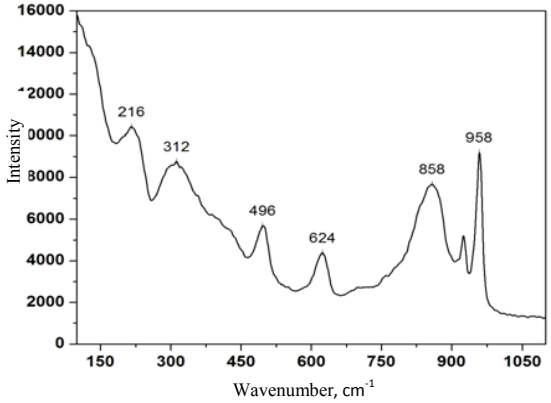

Figure 3. Raman Spectra of zinc vanadate

SEM studies

The surface morphology of the synthesized nano zinc vanade was examined by SEM measurements. Figure 4(a–b) shows the presence of spherical hollow $Zn_2V_2O_7$ nano clusters with good separation, varying in size between 6.5-20 nm. The composition of obtained $Zn_2V_2O_7$ was analyzed by energy dispersive X-ray analysis (EDX). As shown in Figure 5, the EDX result showed the presence of Zn, O and V by the appearance of Zn, O and V peaks without any other characteristic peaks. Hence, the samples $Zn_2V_2O_7$ and do not contain any other element and are indeed free from impurities.

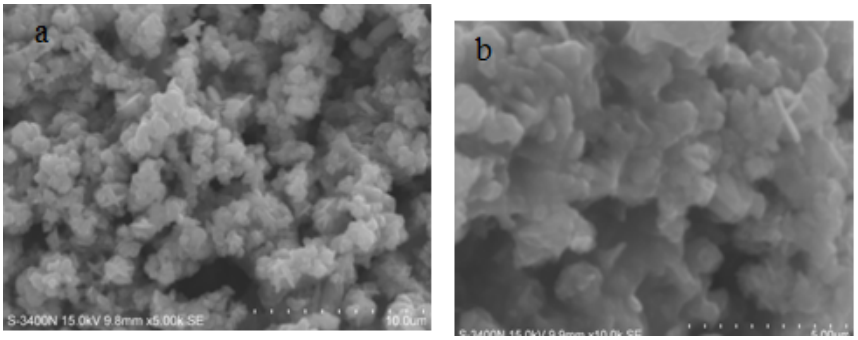

Figure 4(a, b). HR-SEM images of nano zinc vanadate

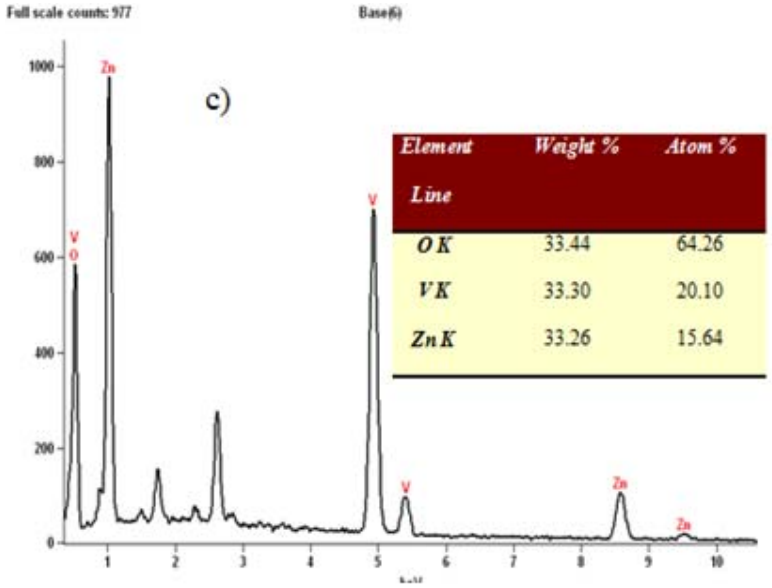

Element Line	Weight %	Atom %
O K	33.44	64.26
V K	33.30	20.10
Zn K	33.26	15.64

Figure 5. EDX Spectrum of nano zinc vanadate

Optical studies (Diffused deflectance spectroscopy)

The energy band gap of nanocrystalline zinc vanadate microspheres was obtained from the optical diffuse reflectance spectra (UV-DRS) at room temperature and is shown in Figure 6. It displays an absorption inflection point at around 385 nm, which should be assigned to the excitonic absorption feature of $Zn_2V_2O_7$. The direct band gap calculated from diffused

reflectance spectra is 3.23 eV, which is higher for nano zinc vanadate than that for bulk zinc vanadate.[11] The increment of the values of optical band gap arises due to improvement in the crystallinity of during annealing treatment.[9,18]

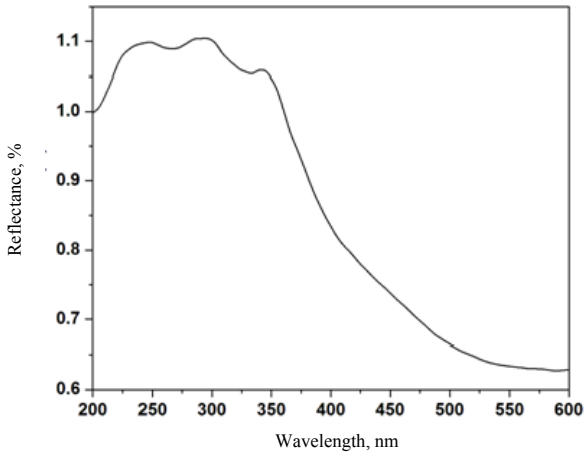

Figure 6. UV-Visible diffuse reflectance spectra of zinc vanadate

Photoluminescence (PL) studies

The photoluminescence (PL) spectra of zinc vanadate nanosphere shown in Figure 7 were recorded for two main reasons: the quantum size effect and structural defects in the crystals. The intense peak obtained at 430 nm is due to the combination of the electrons from the conduction band and holes from the valence band. It was reported that depending on the particle size and exciting wavelength, the different emission peaks could be seen in the range of 400–600 nm peaks[23,25]. The peak observed at 476.5 nm corresponds to the band edge emission for zinc vanadate nanosphere.[25] The band at 533 nm is assigned to near band-gap radiative combination[23]. The emission peak at 520 nm is due to the near band edge emission of zinc vanadate nanosphere. The strong emission peak at 520 nm, suggest that the zinc vanadate nanosphere can be useful in optical material of high quality monochromatic laser[24].

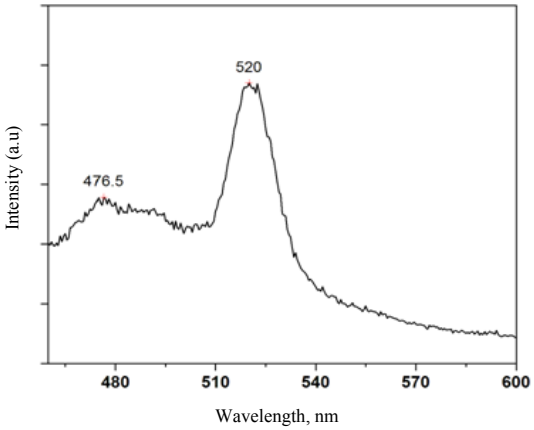

Figure 7. Photoluminescence spectra of zinc vanadate

Photocatalytic studies

Effect of photocatalyst dosage on the photodegradation of MG

The effect of the amount of $Zn_2V_2O_7$ on the photodegradation of MG versus time is shown in Figure 8 & 9. There is decrease of samples absorbance due to the decrease of dye concentration. Since there were no additional peaks appearing in the UV-Vis spectra, it is clear that the dye has been completely degraded. It was observed that the degradation percentage increased with increasing the mass of photocatalyst, reached the higher value (50 mg/100 mL of the photocatalyst) and then decreased due to turbid nature of catalyst with dye. The enhancement of photodegradation efficiency of the dyes with increasing the mass of photocatalyst may be attributed to the rapid transfer of the photo-generated electrons resulting in the effective separation of the electrons and holes[26].

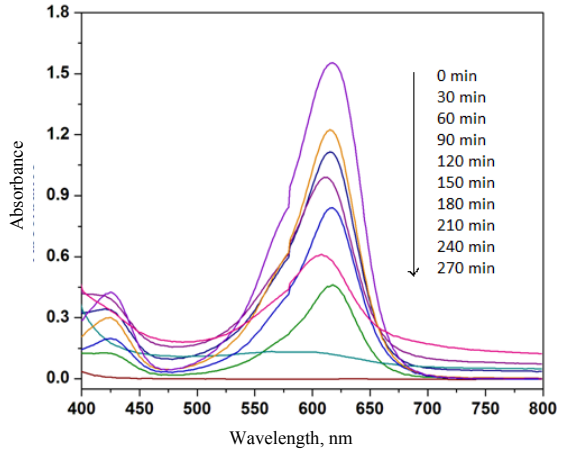

Figure 8. Change in absorbance spectra of MG with the illumination time for the zinc vanadate. Curves 1-9 shows the absorbance spectra after 0, 30, 60, 90, 120, 240 and 270 minute of UV irradation

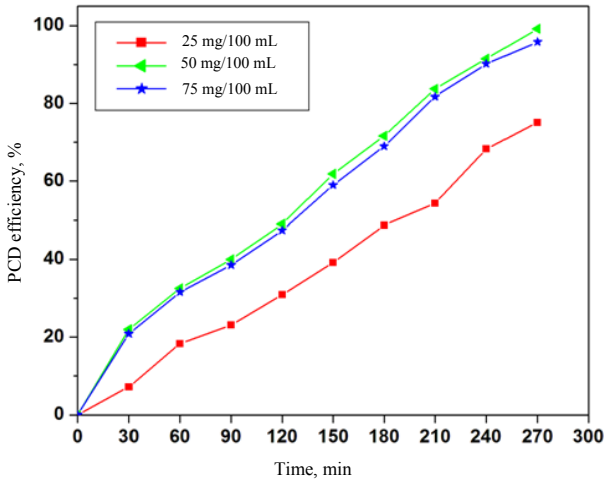

Figure 9. Efftect of photocatalyst dosage on the degradation efficiency, initial MG concentration, 20 mg/L at pH 5.5-6

Effect of the initial dye concentration on the photodegradation of MG

After optimizing the photocatalyst dosage, the effect of initial dye concentration 20 and 40 mg /L on the photodegradation of MG was investigated. The obtained results are shown in Figure 10. It has been observed that the rate of photodegradation for 20 mg/ L is higher. This is because more dye molecules were available for consecutive degradation. The rate of photodegradation was found to decrease with increasing in dye concentration above 20 mg/L. The reason for this decrease is attributed to the shielding effect of dye at high concentration that retards the penetration of light to the dye molecules deposited over catalyst surface. The degradation of MG 20 is also performed in the absence of catalyst (photolysis) and is shown in same figure.

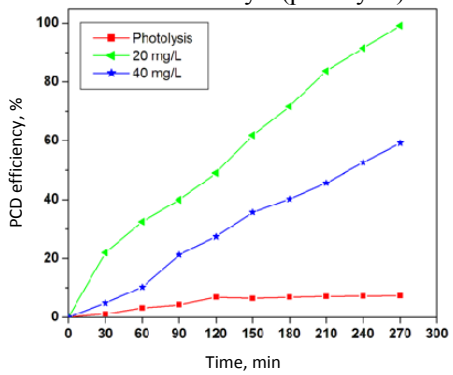

Figure 10. Efftect of the inital concentration of MG on the degradation efficiency, 50 mg/L of the catalyst; initial solution at pH 5.7

Conclusion

$Zn_2V_2O_7$ nanosphere clusters have been successfully synthesized by a simple and rapid microwave-assisted combustion method using diethylene glycol as the fuel. XRD, FT-IR and Raman spectral data confirmed the formation of nano zinc vanadate phase. The formation of nano clusters with web like network around them is shown by SEM. The purity of the synthesised nano vanadate is confirmed by EDX analysis. The direct band gap calculated from diffused reflectance spectra about 3.23eV and the synthesized zinc vanadate nanospheres showed good optoelectronic properties. This synthesis process is an economical and rapid for the preparation of monoclinic structure nano zinc vanadate with respect to energy, time and simplicity. $Zn_2V_2O_7$ spherical cluster shaped nanocrystals showed enhanced photocatalytic activity against 20 mg/ L of MG at 365 nm. The 50 mg/100 mL of $Zn_2V_2O_7$ sample functioned optimally by separating photogenerated electron–hole pairs efficiently. The complete photodegradation of MG was achieved (~99.6), after 270 minutes for the above optimising condition.

Acknowledgements

The authors duly acknowledge and thank Nano tech lab, Noorul Islam University, India and Catalysis and Nanomaterials Research Laboratory, Department of Chemistry, Loyola College, Chennai, India.

References

1. Xu L, Ding Y S, Chen C H, Zhao L L, Rimkus C, Joesten R and Suib S L, *Chem Mater.,* 2008, **20(1)**, 308-316; DOI:10.1021/cm702207w
2. Xia Y, Yang P, Sun Y, Wu Y, Mayers B, Gates B, Yin Y, Kim F and Yan H, *Adv Mater.,* 2003, **15(5)**, 353-389; DOI:10.1002/adma.200390087

3. Zhang J, Lingdong S, Jialu Y, Huilan S, Chunsheng L and Chunhua Y, *Chem Mater.*, 2002, **14(10)**, 4172-4177; DOI:10.1021/cm020077h
4. Geng J, Lu D, Zhu J J and Chen H Y, *J Phys Chem B*, 2006, **110(28),** 13777-13786; DOI:10.1021/jp057562v
5. Mohameda R M, McKinney D L and Sigmund W M, *Mater Sci Eng R.*, 2012, **73(1)**, 1-13; DOI:10.1016/j.mser.2011.09.001
6. Mohamed H H and Bahnemann D W, *Appl Catal B: Environ.*, 2012, **128()**, 91-104; DOI:10.1016/j.apcatb.2012.05.045
7. Bouberki R, Beji Z, Elkabous K, Herbst F, Viau G, Ammar S, Fievet F, Mauger A and Bardeleben J H V, *Chem Mater.*, 2009, **21(5),** 843-855; DOI:10.1021/cm802605u
8. Clament Sahaya Selvam N, Thinesh Kumar R, Yogeenth K, John Kennedy L, Sekaran G and Judith Vijaya J, *Powder Technol.*, 2011, **211(2-3)**, 250-265; DOI:10.1016/j.powtec.2011.04.031
9. Gotic M, Music S, Ivanda M, Soufek M and Popovic S, *J Mole Struct.*, 2005, **744-747**, 535-540; .DOI:10.1016/j.molstruc.2004.10.075
10. Sonali A Mahapure, Vilas H Rane and Jalindar D Ambekar, Latesh K Nikam, Marimuthu R, Milind V Kulkarni and Bharat B Kale, *Mater Res Bull*., 2011, **46(5)**, 635-638; DOI:10.1016/j.materresbull.2011.02.005
11. Ch.V Subba Reddy, In-Hyeong Yeo and Sun-il Mho, *J Phys Chem Solids,* 2008, **69(5-6),** 1261-1264; DOI:10.1016/j.jpcs.2007.10.072
12. Ghosh M and Rao C N R, *Chem Phys Lett.*, 2004, **393(4-6)**, 493-497; DOI:10.1016/j.cplett.2004.06.092
13. Aruna S T and. Mukasyan A S, *Current Opinion in Solid State Mater Sci.*, 2008, **12(3-4)**, 44-50; DOI:10.1016/j.cossms.2008.12.002
14. Koseoglu Y, *Ceram Int.*, 2013, **39(4),** 4221-4230; DOI:10.1016/j.ceramint.2012.11.004.
15. Bhatte K D, Sawant D N, Watile R A and Bhanage B M, *Mater Lett.*, 2012, **69,** 66-68; DOI:10.1016/j.matlet.2011.10.112
16. Sutton W H, *American Ceramic Society Bulletin*, 1989, **68(2),** 376-386.
17. Clament Sagaya Selvam N, Judith Vijaya J and. John Kennedy L, *J Colloid Interface Science*, 2013, **407**, 215-224; DOI:10.1016/j.jcis.2013.06.004
18. Guclu G, Gurdag G and Ozgumus S, *J Appl Polym Sci.,* 2003, **90(8)**, 2034-2039; DOI:10.1002/app.12728
19. Gupta V K and Suhas, *J Environ Manag.,* 2009, **90(8)**, 2313-2342; DOI:l0.1016/j.jenvman.2008.11.017
20. Abd El-Latif M M and Elkady M F, *Desalination,* 2011, **271(1-3)**, 41-54; DOI:10.1016/j.desal.2010.12.004
21. Corma A, López Nieto J M, Paredes N, Perez M, Shen Y, Cao H and Suib S L, *Stud Surf Sci Catal.*, 1992, **72**, 213-220; DOI:10.1016/S0167-2991(08)61673-0
22. Baskoutas S, Giabouranis P, Yannopoulos S N, Dracopoulos V, Toth L, Chrissanthopoulos A and Bouropoulos N, *Thin Solid Films,* 2007, **515(24),** 8461-8464; DOI:10.1016/j.tsf.2007.03.150
23. Yang Z X, Zhong W, Yin Y X, Du X, Deng Y, Au C and Du Y, *Nanoscale Res Lett.*, 2010, **5,** 961-965; DOI:10.1007/s11671-010-9589-y
24. Dong D and Zhu C, *Opt Mater.*, 2003, **22(3)**, 227-233; DOI:10.1016/S0925-3467(02)00269-0
25. Antonietti M and Ozin G A, *Chem Eur J.,* 2004, **10(1)**, 28-41; DOI:10.1002/chem.200305009
26. Stafford U, Gray K A and Kamat P V, *J Catal.,* 1997, **167(1),** 25-32; DOI:10.1006/jcat.1997.1511